UDK: 621.312.22.094.64
COSATI: 01-03, 20-04

Computational Analysis of Helicopter Main Rotor Blades in Ground Effect

Zorana Trivković[1)]
Jelena Svorcan[1)]
Marija Baltić[1)]
Dragan Komarov[1)]
Vasko Fotev[1)]

Numerical investigation of an isolated representative helicopter main rotor has been performed in ANSYS FLUENT 16.2. In general, flow field around the rotor is unsteady, three-dimensional, complex and vortical. Such a simulation requires substantial computational resources. Ground effect, which improves the aerodynamic performances of the rotor, represents an additional challenge to numerical modeling. In this study, flow field is computed by Unsteady Reynolds Averaged Navier-Stokes (URANS) equations. Both Frame of reference and Sliding mesh approaches were employed to model the rotor rotation. Obtained results are compared to results obtained by simpler, sufficiently reliable models such as Momentum Theory (MT) and Blade Element Momentum Theory (BEMT). Presented results include fluid flow visualizations in the form of pressure, velocity and vorticity contours and the values of aerodynamic coefficients.

Key words: **helicopter, helicopter rotor, blades, flow field, Navier-Stokes equations, Reynolds number, aerodynamic coefficients, ground effect.**

Introduction

FLOW field around helicopter blades is highly complex [1-6]. Although many flow phenomena are present (e.g. unsteadiness, tip vortex formation, 3D dynamic stall, blade-vortex interaction, shock/boundary-layer interaction etc.) [5], because of the unique characteristics of helicopters, extensive experimental and numerical research is constantly being conducted for the purpose of improvement of their aerodynamic performances. Several world-wide projects, e.g. HELISHAPE, HART II, GOAHEAD, have been performed in the last two decades [2-6].

Since hover is the basic, the simplest and the most important flight regime of a helicopter, hover performances are an extremely important issue in the helicopter design process ("a dimensioning condition" as stated in [3]). Obtaining a usable, sufficiently accurate numerical solution is a difficult task [3]. There exist several models with different complexity, that can be used for simulation of axis-symmetric flow field in hover and vertical flight. They include momentum models, combined blade-element-momentum models and full Navier-Stokes equations capable of capturing the changes of flow quantities along the blade.

Compared to hover, forward flight regime is even more complicated. Rather than being axis-symmetric, the flow field is quite irregular over the rotor disc, and variations of flow quantities per angular coordinate also exist.

Another interesting phenomenon is that the thrust of a helicopter rotor, operating at constant power, increases as it approaches the ground, since the development of the rotor wake is constrained [1, 7]. Such an effect is extremely important when determining rotor performances and has been studied both experimentally and numerically [7-9] but is still not fully understood [1].

Because of the great complexity of the problem in question, several simplifications of the study had to be adopted. Although the aspect ratio is high for the helicopter blades, they were considered rigid. The coning angle of the blades (as a consequence of mutual aerodynamic and inertial loads) was neglected. The collective pitch, necessary for achieving different values of thrust, was estimated by BEMT. The effect of helicopter fuselage was implicitly included in forward flight computation through necessary values of the angle-of-attack. Unfortunately, these limitations make comparison to the experimental data more difficult and less accurate.

The paper is structured as follows. A short description of the representative rotor used in computations is given in the next section. This is followed by a short description of the used analytical and numerical models, and adopted numerical set-up. The results for both hover and forward flight condition are presented in the section "Results and discussion". In the end, short concluding remarks are given.

Model description

The representative model of a main helicopter rotor was taken from [2] where a description of a conducted experimental investigation on performances of two different rotors, baseline and BERP-type, in the Langley Transonic Dynamics Tunnel (TDT) can be found. The experimental

[1)] University of Belgrade, Faculty of Mechanical Engineering, Kraljice Marije 16, 11020 Belgrade 35, SERBIA
Correspondence to: Zoran Trivković; e-mail: zposteljnik@mas.bg.ac.rs

data, obtained in hover and forward flight over a nominal range of advance ratios from 0.15 to 0.425, were used for validation of the numerical models.

Representative main rotor model consists of 4 rectangular, 1.428m long blades. Blades use two U.S. airfoils: 10% thick RC(4)-10 ($r/R \leq 0.84$) and scaled 8% thick RC(3)-08 ($r/R \geq 0.866$), Fig.1. A smooth transition is made between these two different airfoil shapes. Solidity of the rotor is $\sigma = 0.101$. Twist distribution is triple linear, Fig.2.

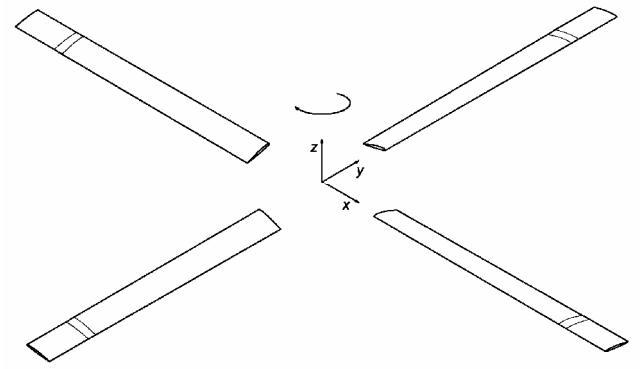

Figure 1. Main rotor model

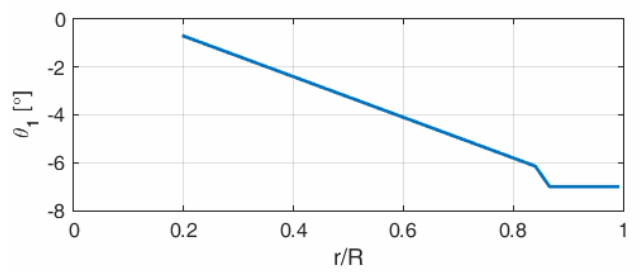

Figure 2. Twist distribution

Nominal test conditions are defined by the advance ratio μ, tip Mach number M_T (constantly kept at 0.628), rotor-shaft angle-of-attack α and blade collective pitch angle θ. Since the values of the last two angles were not known, they were estimated by BEMT. In hover ($\mu = 0$), data were obtained at $z/d = 0.83$ where z is the distance from wind-tunnel floor to rotor hub. Numerical simulations were also performed for another, smaller relative distance $z/d = 0.25$ and the two sets of data were compared.

Numerical approach

As previously stated, since no set of data is complete and the detailed information cannot be provided in a short amount of time, several different analytical and numerical approaches, ranging from fast approximate to high-fidelity, were applied.

Momentum Theory (MT)

Detailed equations can be found in [1]. Conservation laws are applied in a quasi-one-dimension integral formulation to a control volume surrounding the rotor and its wake. This simple approach enables a first level analysis of the rotor thrust and power without the need for consideration of blade characteristics. In modified MT, actual power required to hover presents the sum of induced and profile power:

$$C_P = C_{P_i} + C_{P_0} = \frac{\kappa C_T^{3/2}}{\sqrt{2}} + \frac{\sigma C_{d_0}}{8}. \quad (1)$$

Power can be obtained from required power coefficient as $P = C_P \rho \Omega^2 R^5 \pi$, and thrust as $T = C_T \rho \Omega^2 R^4 \pi$ where ρ is air density and Ω rotor angular velocity.

In forward flight, due to forward speed and existence of fuselage, additional members appear:

$$C_P = \kappa \lambda C_T + \frac{\sigma C_{d_0}}{8}\left(1 + 4.65\mu^2\right) + \frac{1}{2}\left(\frac{f}{A}\right)\mu^3. \quad (2)$$

Although this model assumes uniform distribution of flow quantities across disc rotor, by "correctly" estimating the values of induced power correction factor κ, section profile drag coefficient C_{d0} and fuselage equivalent wetted area f, it is possible to obtain sufficiently accurate estimations of required power coefficient. Here, these values were adopted in accordance with the available experimental data.

By replacing the rotor with a simple source, with an image source to simulate the ground effect [7], for constant power, ratio of thrust in (IGE) and out of ground effect (OGE) in hover can be presented by the corresponding ratio of induced velocities. Assuming uniform distributions over the rotor area, the equation becomes:

$$\left[\frac{T_{IGE}}{T_{OGE}}\right]_{P=const.} = \frac{1}{1-(R/4z)^2} \quad (3)$$

where R is rotor radius and z is rotor height off the ground.

Blade Element Momentum Theory (BEMT)

This hybrid approach combines the basic principles from both the blade element and the momentum theory. As a result, if the blade twist distribution is known, it is possible to solve the induced velocity distribution. Afterwards, with the known airfoil aerodynamic characteristics, it is possible to estimate thrust and power increments along the blade. However, these integrals become quite complicated for forward flight and here this approach was used only for hover.

Necessary airfoil aerodynamic characteristics were taken from [10, 11].

To account for the ground effect in hover, the BEMT results were corrected according to [1]:

$$C_P = k_G C_{P_i} + C_{P_0}, k_G = \frac{1}{0.9926 + 0.0379(2R/z)^2}. \quad (4)$$

Unsteady Reynolds Averaged Navier-Stokes equations (URANS)

Since two different distances from ground were considered ($z/d = 0.25$ and $z/d = 0.83$) at several different thrust coefficients (different pitch distributions), several different computational grids had to be created. All generated meshes are unstructured, three-dimensional and prismatic extending from -0.83 (-0.25) to 1.5 rotor diameters along the z-axis and 5 blade lengths in both x- and y-directions, Fig.3. They contain two fluid zones, rotor and stator, and a total number of cells of approximately 2 million. This number was adopted after a grid convergence study. Meshes are additionally refined around the blades, Fig.4. Dimensionless wall distance around the blades is below 5, $y^+ < 5$. Trailing edge of the blades is modeled as blunt.

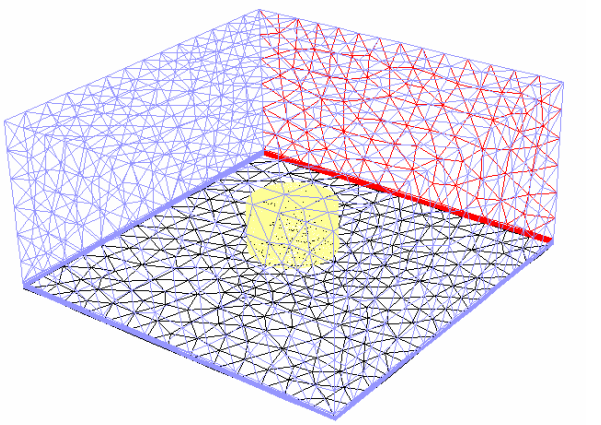

Figure 3. Example of a generated mesh; blue - pressure inlet, red - pressure outlet, black - ground, yellow - interface between rotor and stator

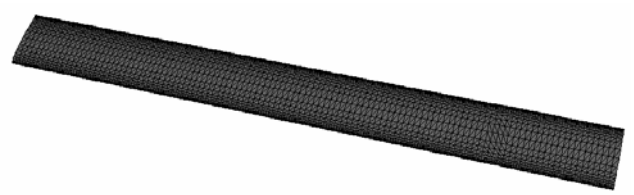

Figure 4. Mesh along the blade surfaces

In order to decrease the number of cells and better resolve the fluid flow it is customary to generate only a part of the mesh around a single blade and define periodic boundary conditions at the sides. This approach is particularly applicable in axis-symmetric hover and vertical flight conditions. However, since in this study forward flight condition was also considered, complete meshes were generated and used for both flight cases.

Apart from the computational grid appearance, flight condition also dictates the numerical approach. Isolated rotor in hover and vertical flight can successfully be simulated by steady flow in a rotating frame of reference while the forward flight condition is better represented by moving meshes since periodic unsteadiness during one rotation can be more accurately captured. Here, both approaches were used.

Dirichlet boundary conditions concerning velocity and pressure were imposed on inlet and outlet boundaries. No-slip boundary conditions were defined on blade and floor surfaces. Angular velocity of 149rad/s, resulting in fixed M_T, was assigned to rotor zone.

Numerical simulations were performed in ANSYS FLUENT 16.2 where governing flow equations for compressible, viscous fluid were solved by finite-volume method. Unsteady Reynolds-averaged Navier-Stokes (URANS) equations were closed by a two-equation k-ω SST turbulence model. Fluid, air, was considered as ideal gas whose dynamic viscosity changes according to the Sutherland law.

Pressure-based coupled solver was used. Gradients were obtained by the least squares cell-based method. Spatial discretizations were of the second order. Where needed (unsteady simulations of isolated rotor in forward flight), temporal discretization was of the first order. Courant-Friedrichs-Lewy (CFL) number was in the range 1-5.

Results and discussion

Obtained results are grouped in accordance with the flight condition. Rotor hover performance was computed at 5 different collective angles. Tip Mach number was kept constant in all performed simulations.

Hover

Obtained relations between thrust coefficient C_T and required power coefficient C_P at $z/d = 0.83$ and $z/d = 0.25$ are presented in Figures 5 and 6 respectively.

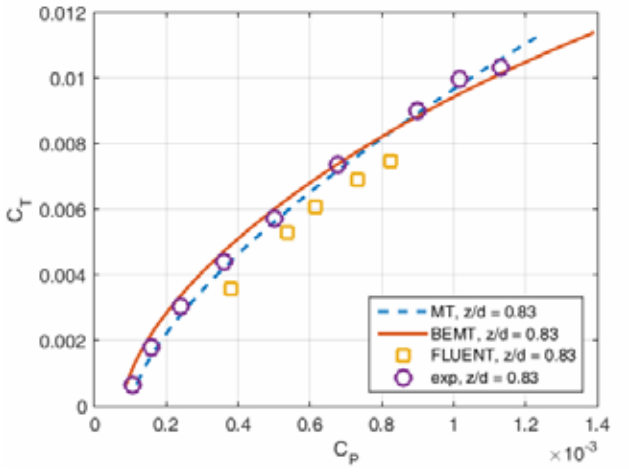

Figure 5. $C_P = f(C_T)$ at $z/d = 0.83$

Although experimental data is available only for $z/d = 0.83$, all numerical models clearly capture the increase in aerodynamic performances in ground vicinity, i.e. for the same thrust less power is required. BEMT results very well correspond to the experimental data. FLUENT results somewhat underestimate the rotor performance although the character of the relation C_P-C_T is accurately captured. This small discrepancy can, at least partially, be explained by the existence of wind tunnel walls (not present in numerical model). Another explanation may be the numerical set-up, i.e. mesh density, turbulence model, the use of the steady frame of reference approach, etc.

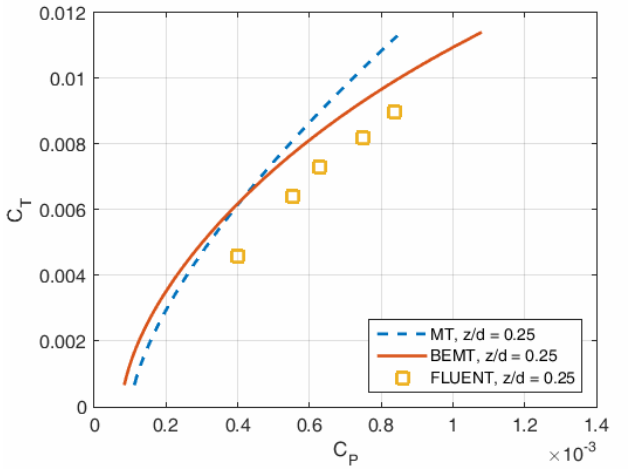

Figure 6. $C_P = f(C_T)$ at $z/d = 0.25$

Numerical results obtained in FLUENT can also be validated against a known relation marked as eq. 3, Fig.7. A plot of the thrust ratio in hover versus relative height from the ground has been drawn for different geometries (i.e. different collective pitch angles θ). Although small deviations exist (in particular for higher collective pitch angles), it can be concluded that the trend of the change has been successfully captured. The ground effect is particularly important for $z/R < 1$, i.e. $z/d < 0.5$.

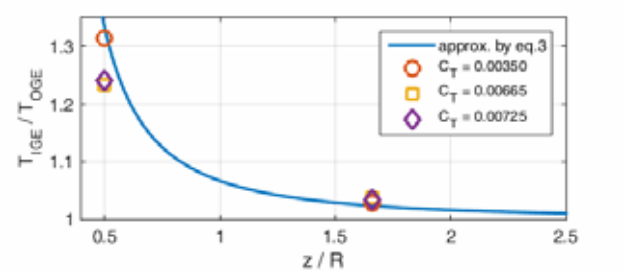

Figure 7. $T_{IGE}/T_{OGE} = f(z/R)$ for different geometries

An illustrative comparison of fluid flows at two different distances from the ground can be made by comparing pressure coefficients C_p along two spanwise locations on the blade, r/R = 0.775 and r/R = 0.945, for a single geometry (collective angle), Fig.8.

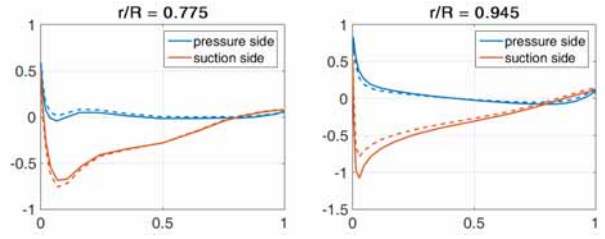

Figure 8. Chordwise C_p distributions at 2 cross sections for one collective angle at z/d = 0.83 (-) and z/d = 0.25 (--)

Full line denotes z/d = 0.83, while dashed line refers to z/d = 0.25. Although no experimental data is available for the comparison, computed plots are consistent with results obtained by other authors [5, 12]. Greater pressure difference, resulting in increased thrust is evident for z/d = 0.25 at inner parts of the blade. Near the blade tip, for smaller z the velocity increases and pressure decreases.

Behavior of the wake from the hovering rotor in ground effect can be presented by streamlines, Fig.9. Slipstream expansion near the surface is obvious.

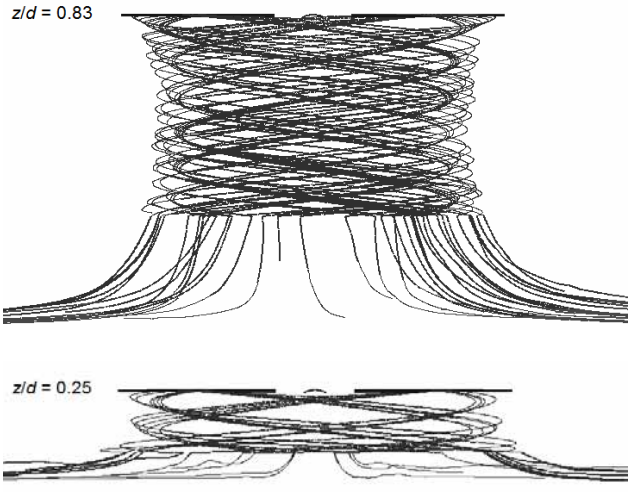

Figure 9. Streamlines from the hovering rotor for one collective angle at z/d = 0.83 and z/d = 0.25

Flow field is affected by the vicinity of the ground, both slipstream and induced velocities change, resulting in altered power and thrust coefficients. These changes can also be illustrated by vorticity fields, Fig.10.

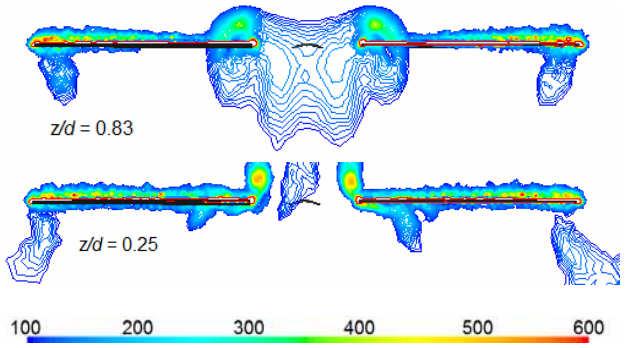

Figure 10. Vorticity contours in [s^{-1}] in midplane for one collective angle at z/d = 0.83 and z/d = 0.25

Forward flight

The ground effect on rotor performance in forward flight is also important. However, the flow field around the rotor gets even more complicated [1]. Flow characteristics also greatly depend on the forward speed, i.e. advance ratio μ, and for the same geometry (collective angle) thrust coefficient increases in forward flight when compared to hover. For that reason, forward flight simulations were performed on 3 different model geometries, for two distances from the ground z/d = 0.83 and z/d = 0.25, and a single advance ratio μ = 0.1.

In order to accurately simulate forward flight condition, it was necessary to use sliding mesh approach. Pressure far-field boundary conditions defining values of pressure, velocity and turbulence quantities were assigned to outer domain surfaces. Time step corresponds to an angular increment of 5°. A great number of rotations (around 10), was necessary for attaining quasi-convergence of thrust and power coefficients.

Results computed in ANSYS FLUENT, marked by square symbols in Figures 11 and 12, were compared to experimental data (where available) and MT results. Again, power coefficients computed by URANS are somewhat higher than those by MT, and both sets of numerical results seem higher than the experimental values. However, the character of the relations seems to be well captured, although discrepancies increase with the increase of advance ratio (i.e. for μ = 0.1). Ideally, for thorough analysis, a complete map of aerodynamic performances should be generated (for various μ and θ). However, since the simulations require large amounts of time, at this stage of the study, only individual results are presented (as discrete points on the graphs). One color refers to a single value of thrust coefficient.

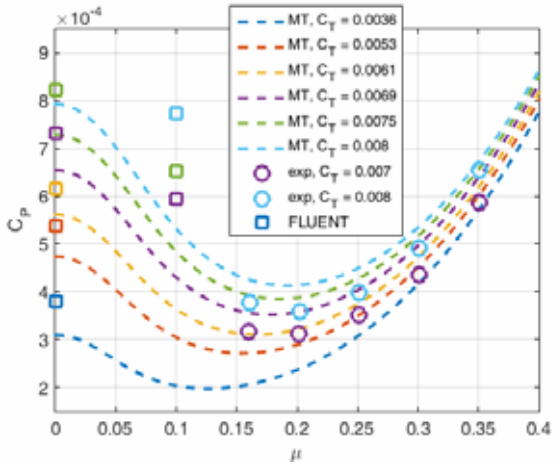

Figure 11. $C_P = f(\mu)$ at z/d = 0.83

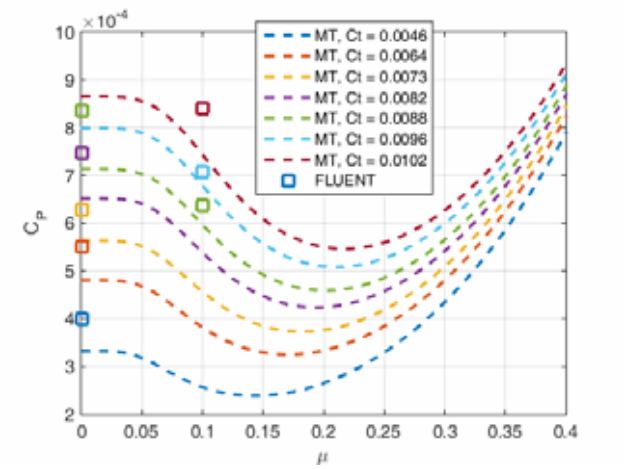

Figure 12. $C_P = f(\mu)$ at $z/d = 0.25$

Although thrust coefficients are different, smaller amounts of required power at the lower distance from the ground ($z/d = 0.25$) for low advance ratios are evident (i.e. for the same C_P much higher C_T can be achieved). Unfortunately, no experimental data is available for the employed model of the helicopter rotor at low advance ratios.

Blade sectional pressure coefficients at the radial positions $x/R = 0.775$ and $x/R = 0.945$ during one revolution with the angular increment of $\Delta\psi = 60°$ are presented in Figures 13 and 14 respectively. Full line denotes $z/d = 0.83$ and dashed line refers to $z/d = 0.25$. Again, computed results are comparable with the other published results [6, 13]. Since the advance ratio is low, the overall flow variations are smaller at the inner part of the blade.

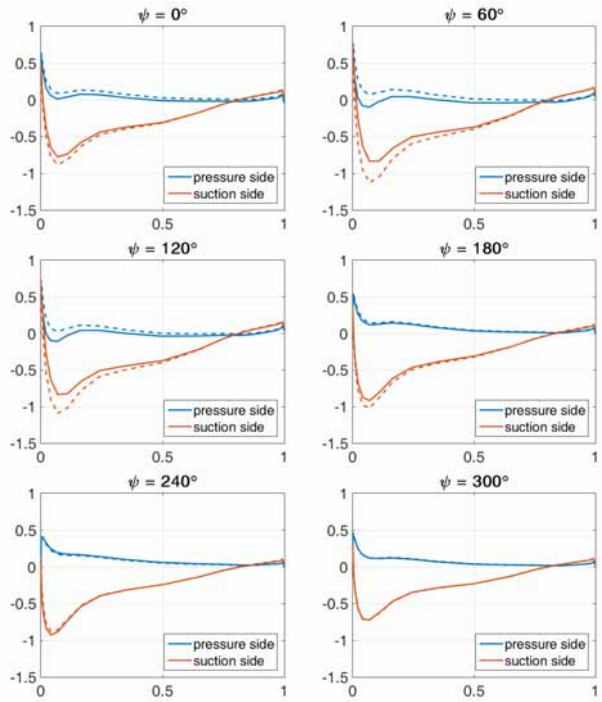

Figure 13. Chordwise C_p distributions at $x/R = 0.775$

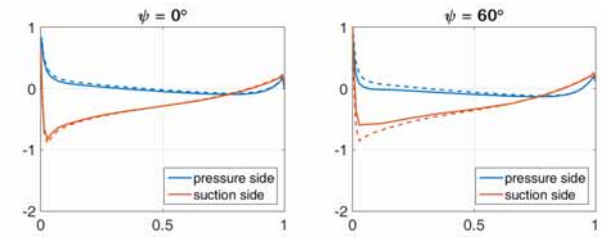

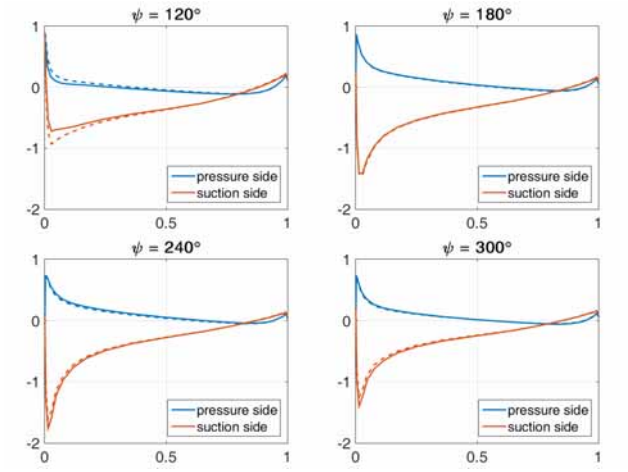

Figure 14. Chordwise Cp distributions at $x/R = 0.945$

Main differences in the two ground distances can primarily be seen at the advancing side of the rotor. At the retreating side, pressure distributions seem quite similar.

Flow structures in slow forward flight can be illustrated by streamlines, Fig.15. Region of flow recirculation formed upstream of the rotor at $z/d = 0.25$ is noticeable. Employed CFD solver seems able to reproduce the transient flow and loading of the blade.

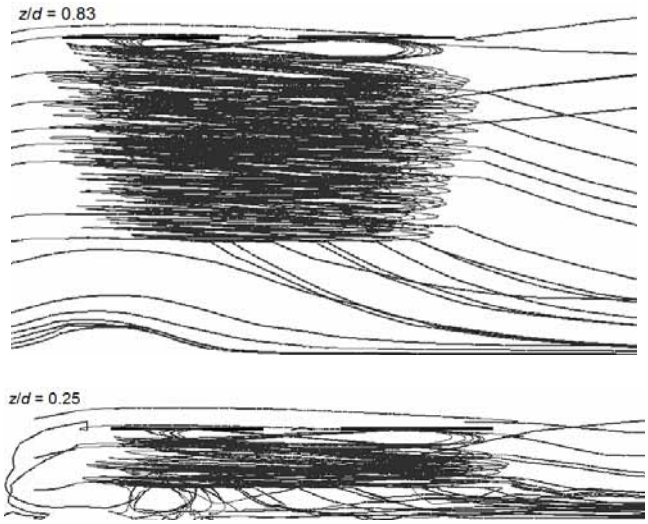

Figure 15. Streamlines from the rotor in forward flight for one collective angle at $z/d = 0.83$ and $z/d = 0.25$

Conclusion

Aerodynamic performances of an isolated model helicopter main rotor in ground effect (at two distances from the ground) obtained by several different analytical and numerical approaches, ranging from fast approximate to high-fidelity detailed solutions, were compared. For the most cases, satisfactory outcome (agreement with experimental data) was accomplished, given the fact that relatively limited success has been achieved in correctly predicting rotor performance in ground effect when compared to the experimental results [1]. This is due to the problem complexity and strongly viscous nature of the rotor IGE problem.

None of the employed numerical models can fully capture the complexity of the flow. However, through their combination and comparison with available experimental data many useful pieces of information can be extracted.

Presented results have contemporary importance and enable the development of a more efficient rotor design. They also provide insight into complex flow fields around a representative rotor in hover and forward flight (two quite different, but equally important flight regimes). Although an additional work is necessary, it is possible to use the presented numerical set-ups to assess the possible increase of aerodynamic performances in ground effect.

Acknowledgement

The paper is a contribution to the research TR 35035 in 2016, funded by the Ministry of Education, Science and Technological Development of the Republic of Serbia.

References

[1] LEISHMAN,J.G.: *Principles of Helicopter Aerodynamics*, 2nd ed., Cambridge University Press, New York, 2006.

[2] YEAGER,W.T.Jr., NOONAN,K.W., SINGLETON,J.D., WILBUR,M.L., MIRICK,P.H.: *Performance and Vibratory Loads Data from a Wind-Tunnel Test of a Model Helicopter Main-Rotor Blade with a Paddle-Type Tip*, NASA TM 4754, Hampton, Virginia, 1997.

[3] POMIN,H., ALTMIKUS,A., BUCHTALA,B., WAGNER,S.: *Rotary Wing Aerodynamics and Aeroelasticity*, in High performance Computing in Science and Engineering 2000, Springer-Verlag Berlin Heidelberg, 2001.

[4] BEAUMIER,P., BOUSQUET,J.-M..: *Applied CFD for analyzing aerodynamic flows around helicopters*, 24th International Congress of the Aeronautical Sciences, Yokohama, Japan, 2004.

[5] BARAKOS,G., STEIJL,R., BADCOCK,K., BROCKLEHURST,A.: *Development of CFD capability for full helicopter analysis*, 31st European Rotorcraft Forum, Florence, Italy, 2005.

[6] ANTONIADIS,A.F., DRIKAKIS,D., ZHONG,B., BARAKOS,G., STEIJL,R, BIAVA,M. et al.: *Assessment of CFD methods against experimental flow measurements for helicopter flows*, Aerospace Science and Technology, 2012, 19, pp.86-100.

[7] CHEESEMAN,I.C., BENNETT,W.E.: *The Effect of the Ground on a Helicopter Rotor in Forward Flight*, R. & M. No. 3021, London, 1957.

[8] GANESH,B.: *Unsteady Aerodynamics of Rotorcraft at low Advance Ratios in Ground Effect*, Ph.D. thesis, Georgia Institute of Technology, 2006.

[9] PULLA,D.P.: *A study of helicopter aerodynamics in ground effect*, Ph.D. thesis, The Ohio State University, 2006.

[10] BINGHAM,G.J., NOONAN,K.W.: *Two-Dimensional Aerodynamic Characteristics of Three Rotorcraft Airfoils at Mach Numbers from 0.35 to 0.90*, NASA TP 2000, Hampton, Virginia, 1982.

[11] NOONAN,K.W.: *Aerodynamic Characteristics of Two Rotorcraft Airfoils Designed for Application to the Inboard Region of a Main Rotor Blade*, NASA TP 3009, Hampton, Virginia, 1990.

[12] JARKOWSKI,M., WOODGATE,M.A., BARAKOS,G.N., ROKICKI,J.: *Towards consistent hybrid overset mesh methods for rotorcraft CFD*, Int. J. Numer. Meth. Fluids, 2014, 74, pp.543-576.

[13] BIAVA,M., KHIER,W., VIGEVANO,L.: *CFD prediction of air flow past a full helicopter configuration*, Aerospace Science and Technology, 2012, 19, pp.3-18.

Received: 30.03.2016.
Accepted: 07.10.2016.

Numerička analiza lopatica glavnog rotora helikoptera u blizini zemlje

Numerička analiza izolovanog, reprezentativnog glavnog rotora helikoptera izvršena je u komercijalnom softverskom paketu ANSYS FLUENT 16.2. Generalno, strujna slika oko rotora je nestacionarna, trodimenzionalna, složena i vrtložna. Takve simulacije zahtevaju značajne proračunske resurse. Uticaj zemlje, koji poboljšava aerodinamičke performanse rotora, predstavlja dodatni izazov pri numeričkom modeliranju. U ovom radu strujno polje je izračunato Navije-Stoksovim jednačinama osrednjenim Rejnoldsovom statistikom (RANS). Rotaciono kretanje uzeto je u obzir primenom dva različita pristupa: "Frame of reference" i "Sliding mesh". Izvršeno je poređenje dobijenih rezultata sa vrednostima jednostavnijih modela kao što su model zasnovan na zakonima održanja (MT) i kombinovani model segmenta lopatice (BEMT). Rezultati su predstavljenu u obliku kontura pritiska, brzine i vrtložnosti kao i vrednostima aerodinamičkih koeficijenata..

Ključne reči: **helikopter, rotor helikoptera, lopatice, strujno polje, Navije-Stoksove jednačine, Rejnoldsov broj, aerodinamički koeficijenti, uticaj zemlje.**

Численный анализ лопастей несущего винта ротора вертолёта вблизи земли

Численное исследование изолированного представителя несущего винта ротора вертолёта было выполнено в коммерческом комплекте программного обеспечения ANSYS FLUENT 16.2. В общем, поток поля вокруг ротора неустойчив, трёхмерный, сложный и вихревой. Такое моделирование требует значительных финансовых ресурсов. Первый эффект – влияние земли, который улучшает аэродинамические характеристики ротора, представляет собой дополнительную проблему для численного моделирования. В этом исследовании, поле потока вычисляется путём уравнений Навье-Стокса усредненными нестационарной статистикой Рейнольдса (RANS). Обе системы отсчёта и скользящие сетки подхода были использованы для моделирования вращения ротора. Полученные результаты сравнивают с результатами, полученными с помощью более простых, достаточно надёжных моделей, таких как элемент теории импульса (MT) и комбинированная модель лезвия лопастей ротора (BEMT). Представленные результаты включают визуализацию потока текучей среды в виде контуров давления, скорости и завихренности и значения аэродинамических коэффициентов.

Ключевые слова: **вертолёт, несущий винт ротора вертолёта, лопасти, поле потока, уравнения Навье-Стокса, число Рейнольдса, аэродинамические коэффициенты, влияние земли.**

Analyse numériques des aubes du rotor principal d'hélicoptère à proximité du sol

Analyse numérique du rotor principal isolé et représentatif de l'hélicoptère a été faite par le logiciel commercial ANSYS FLUENT 16.2. En général l'image du courant autour du rotor est non stationnaire, à trois dimensions, complexe et tourbillonnante. Les simulations de ce genre demandent des ressources de computation considérables. L'influence du sol qui améliore les performances aérodynamiques de rotor représente un défi additionnel lors de la modélisation numérique. Dans ce travail le champ de courant a été calculé par les équations Navier-Stokes et par les statistiques moyennes de Reynolds (RANS). Le mouvement de rotation a été pris en considération à l'aide de deux approches différentes : « Frame of reference » et « Sliding mash » . On a comparé les résultats obtenus et les valeurs des modèles plus simples tels que le modèle basé sur les lois de survie (MT) et le modèle combiné des éléments de l'aube (BEMT). Les résultats sont présentés en forme de contour de pression, vitesse et tourbillon ainsi que par les valeurs des coefficients aérodynamiques.

Mots clés: **hélicoptère, rotor de hélicoptère, aubes, champ de courant, équations Navier-Stokes, nombre de Reynolds, coefficient aérodynamique, influence du sol.**